J Mater Sci (2007) 42:9245–9255
DOI 10.1007/s10853-007-1911-4

Nanostructured fumed metal oxides for thermal interface pastes

Chuangang Lin · D. D. L. Chung

Received: 20 March 2007 / Accepted: 31 May 2007 / Published online: 27 July 2007

Abstract Fumed metal oxides (13 nm aluminum oxide particles and 20–25 nm zinc oxide particles), which are in the form of porous agglomerates of nanoparticles, are effective as thermally conductive solid components in thermal pastes. They are as effective as carbon black, but are advantageous in their electrical non-conductivity. Without fuming, the oxides are less effective. By coating with silane, which decreases the viscosity of the paste, they are even more effective. The organic vehicle (polyol esters) and solid component content (2.4–4.0 vol.%) are chosen to attain conformability and spreadability. The use of either 4.0 vol.% silane coated fumed zinc oxide or 2.4 vol.% silane coated alumina gives thermal pastes that are more effective than commercial thermal pastes (Ceramique and Shin-Etsu). Fumed zinc oxide is superior to non-fumed zinc oxide in improving the thermal stability. Silane coating of the fumed zinc oxide further improves the thermal stability. Fumed alumina does not affect the thermal stability, but silane coated fumed alumina improves the thermal stability. Though silane coated fumed zinc oxide is superior to silane coated alumina in enhancing the thermal stability, it is slightly inferior in the phase separation tendency.

C. Lin · D. D. L. Chung (✉)
Composite Materials Research Laboratory,
University at Buffalo, State University of New York,
Buffalo, NY 14260-4400, USA
e-mail: ddlchung@eng.buffalo.edu

Introduction

Thermal interface materials [1–6] in the form of thermal pastes are needed to improve thermal contacts, such as that between a microprocessor and a heat sink of a computer. The paste displaces the air from the valleys of the topography of the mating surfaces, which are never perfectly smooth. Since air is thermally insulating, this displacement results in an improved thermal contact. The ability to displace air hinges on the conformability of the thermal paste, i.e., the thermal paste needs to conform to the topography of the mating surfaces. Since the topography is frequently in the microscale, the paste needs to be able to fill valleys in the microscale. In addition, it is preferable that the paste is conductive thermally. Due to the critical importance of microelectronic cooling to the reliability, performance and further miniaturization of computers and other microelectronic systems, the development of thermal interface materials is technologically important. As heat sinks improve, the bottleneck in the heat transfer shifts more and more to the thermal contact. This makes thermal interface materials increasingly important in the overall problem of thermal management in electronic systems.

A thermal paste comprises a vehicle that is filled with a thermally conductive solid. This solid is in the form of particles. The particles should be sufficiently small in size in order to fill the microscale valleys in the surface topography. Thus, nanoparticles are attractive for formulating thermal pastes. Although the thermal conductivity of a thermal paste increases with the conductive solid content, the conformability of the paste decreases with increasing solid content beyond a certain level. In other words, an excessive solid content is detrimental to the conformability of the paste, though it helps the thermal conductivity within the paste [7]. The thermal conductivity within the paste

should be distinguished from the thermal contact conductance across the thermal contact. It is the latter that describes the effectiveness of a thermal paste.

It has been reported that carbon nanoparticles (30 nm) in the form of carbon black provide thermal pastes of high effectiveness [8–12]. Due to the porous agglomerate structure of carbon black, carbon black is highly compressible (squishable). This characteristic helps the attainment of connectivity in a composite material that contains carbon black. Both the nanostructure and squishability of carbon black contribute to the conformability and spreadability of carbon black paste. Although carbon black is much less conductive thermally than silver, carbon black paste can outperform silver paste [9–12]. This is a consequence of the conformability of carbon black paste.

A shortcoming of carbon black is its electrical conductivity. Thermal pastes that are electrically non-conductive are desirable, for fear of causing short-circuiting. Therefore, the development of electrically non-conductive thermal pastes using porous agglomerates of electrically non-conductive nanoparticles (namely, fumed metal oxides [13–15]) is the objective of this paper.

Fumed metal oxides such as fumed alumina have been previously disclosed for use as a minor solid additive (1–5 wt.%) in a thermally conductive paste that contains 60–90 wt.% of a conductive powder (such as silver) [16]. Fumed metal oxides such as fumed alumina have also been disclosed for use as a minor solid additive (0.1–5.0%) in an electrically conductive paste that contains 15–60% of a conductive powder (such as silver) [17]. However, fumed metal oxides have not been previously disclosed for use as the major or sole solid component in a thermally or electrically conductive paste. Furthermore, no paste involving any fumed metal oxide in any proportion has been previously evaluated in terms of its effectiveness as a thermal interface material.

Nanostructured fumed metal oxides include zinc oxide, aluminum oxide, titanium dioxide and silicon dioxide. They are formed by gas-phase reactions. Among these oxides, zinc oxide is particularly attractive, due to its relatively high thermal conductivity. This paper addresses the formulation and performance of thermal pastes that contain a fumed metal oxide as the thermally conductive component. Pastes containing different types of oxide at various volume fractions are compared in terms of the effectiveness as thermal interface materials. In addition, due to the importance of stability at elevated temperatures in practical applications, the pastes are also compared in terms of their thermal stability, as indicated by weight loss measurement.

Experimental methods

Materials

The materials in this study are listed in Table 1. They include fumed and non-fumed metal oxides, in addition to carbon black.

The fumed metal oxides studied are zinc oxide, aluminum oxide and titanium dioxide, which are commercially available. One form of fumed zinc oxide used is VP AdNano Z805 from Degussa AG (Hanau, Germany). It is referred to as "fumed zinc oxide with silane coating". It is a nanostructured zinc oxide that has been treated by the manufacturer with an octylsilanized hydrophobic surface. The zinc oxide content exceeds 99.5%. The carbon content is 0.2–1.0 wt.%. The zinc oxide is a crystalline solid exhibiting the wurtzite structure, just as the naturally

Table 1 Solid components investigated

Description	Commercial designation	Composition/ morphology	Particle size	Surface treatment	Source
Carbon black	XC72R	Carbon black	30 nm	None	Cabot
Fumed alumina 1	SpectrAl 51	Al_2O_3 (fumed)	–	None	Cabot
Fumed alumina 2	ALU C	Al_2O_3 (fumed)	13 nm	None	Degussa
Fumed alumina with silane coating	ALU C805	Al_2O_3 (fumed)	13 nm	Silane coated	Degussa
Non-fumed alumina 1	M300	γ-Al_2O_3	50 nm	None	Metlab Corp.
Non-fumed alumina 2	WCA	α-Al_2O_3	3.2 μm	None	Mico Abrasives Corp.
Fumed zinc oxide	ZnO 20	ZnO (fumed)	25 nm	None	Degussa
Fumed zinc oxide with silane coating	Z 805	ZnO (fumed)	25 nm	Silane coated	Degussa
Non-fumed zinc oxide 1	ZANO 30	ZnO	30 nm	None	Umicore
Non-fumed zinc oxide 2	Kadox 930	ZnO	0.33 μm	None	Zinc Corp. of America
Titanium dioxide	TiO_2 P25	TiO_2 (fumed)	21 nm	None	Degussa

occurring mineral zincite. In this crystal structure, the zinc atom is surrounded tetrahedrally by four oxygen atoms. The smallest units of this material, visible with the electron microscope, are the primary particles of size of the order of 100 nm. The primary particles are joined to each other to form aggregates, which further loosely connect to form agglomerates of size up to 1 mm. The BET specific surface area is 20–25 m^2/g.

Another from of fumed zinc oxide used is VP AdNano ZnO 20 from Degussa AG (Hanau, Germany). It is referred to as "fumed zinc oxide". It is a hydrophilic nanostructured zinc oxide. The fumed zinc oxide Z805 mentioned above is made from this material in a continuous post-treatment process of silanization involving trimethoxyoctylsilane. Thus, the purity and specific surface area are essentially the same for these two types of zinc oxide.

A type of fumed alumina used in this study is Aeroxide ALU C from Degussa AG (Hanau, Germany). It is referred to as "fumed alumina 2". It is aluminum oxide with average particle size 13 nm, BET specific surface area 100 ± 15 m^2/g, Al_2O_3 content at least 96 wt.%, and carbon content 3.0–4.5 wt.%. The Aeroxide ALU C 805 (referred to as "fumed alumina with silane coating") supplied by Degussa in this study was made from fumed alumina 2 by surface treatment with trimethoxyoctylsilane.

Another type of fumed alumina used is SpectrAl 51 from Cabot Corp. (Billerica, MA). It is referred to as "fumed alumina 1". It is in the form of nanoparticles with BET specific surface area 55 m^2/g and Al_2O_3 content exceeding 99.8 wt.%.

The fumed titanium dioxide used is Aeroxide TiO_2 P 25 from Degussa AG (Hanau, Germany), with primary particle size 21 nm, BET specific surface area 50 ± 15 m^2/g, TiO_2 content at least 99.50 wt.%, Al_2O_3 content at or below 0.300 wt.%, SiO_2 content at or below 0.200 wt.%, Fe_2O_3 content at or below 0.010 wt.%, and HCl content at or below 0.300 wt.%.

In order to understand the effect of the particle morphology, the following non-fumed oxides are included in this study: zinc oxide nanoparticles ZANO 30 (Umicore Zinc Chemicals, Angleur, Belgium; referred to as "non-fumed zinc oxide 1"), submicron zinc oxide particles Kadox 930 (Zinc Corporation of America, Monaca, PA; referred to as non-fumed zinc oxide 2"), alumina nanoparticles M300 (Metlab Corporation, Niagara Falls, NY; referred to as "non-fumed alumina 1") and micron-sized alumina particles WCA (Mico Abrasives Corporation, Westfield, MA; referred to as "non-fumed alumina 2").

For the sake of comparison, this study includes carbon black. The carbon black is a type for electrical conductivity and easy dispersion (Vulcan XC72R GP-3820; Cabot Corp., Billerica, MA). It consists of porous agglomerates of carbon particles of particle size 30 nm, density 1.7–1.9 g/cm^3, nitrogen specific surface area 254 m^2/g and maximum ash content 0.2%. It is used in the amount of 2.4 vol.%, which is the optimized amount used in prior work [12].

The morphology of the various oxide fillers is shown by the SEM micrographs in Fig. 1. The fumed oxides exhibit a fluffy porous agglomerate structure, whether the oxide is alumina (Fig. 1a–c) or zinc oxide (Fig. 1e and f).

The vehicle consists of polyol esters, which are attractive for their ability to resist elevated temperatures. The polyol esters in the vehicle are pentaerythritol ester of linear and branched fatty acids and dipentaerythritol ester of linear and branched fatty acids. The polyol ester mixture is Hatcol 2372, as provided by Hatco Corp., Fords, NJ [12]. The specific gravity is 0.97. No solute is used.

All the pastes in this work, regardless of the type of filler, are prepared by ultrasonic dispersion for 10 min with a certain amount of acetone as the solvent, followed by placing the paste in a vacuum chamber (which involves a mechanical vacuum pump) at 70 °C for 24 h for the purpose of solvent removal. Acetone is used as solvent because it greatly reduces the viscosity of the pastes and can be evaporated fast. The uniformity of the mixing is indicated by the consistency of the testing data obtained from various specimens from the same batch of paste.

For the sake of comparison, this study also includes commercial thermal pastes, namely Shin-Etsu X-23-7762 (aluminum particle filled silicone from Shin-Etsu MicroSi, Inc., Phoenix, AZ, with density 2.6 g/ml and thermal conductivity 6.0 W/m K) and Ceramique (density 2.7–2.8 g/ml, in the form of oils containing aluminum oxide, boron nitride and zinc oxide submicron particles, but without metal particles, from Arctic Silver Inc., Visalia, CA).

Testing

Thermal contact conductance measurement

A steady-state method known as the Guarded Hot Plate Method (ASTM Method D5470) is used to measure the thermal contact conductance for various thermal contacts. Various thermal pastes are sandwiched between the 1 × 1 inch (25 × 25 mm) proximate surfaces of two copper blocks (both 1 × 1 inch surfaces of each block having a controlled degree of roughness). Each copper block has a height of 35 mm.

The heat in this test is provided by a 3 × 3 inch (76 × 76 mm) copper block that has two embedded heating coils (top block in Fig. 2). During the period of temperature rise, the heating rate is controlled at 3.2 °C/min by using a temperature controller. This copper block is in contact with one of the 1 × 1 inch copper blocks that sandwiched the

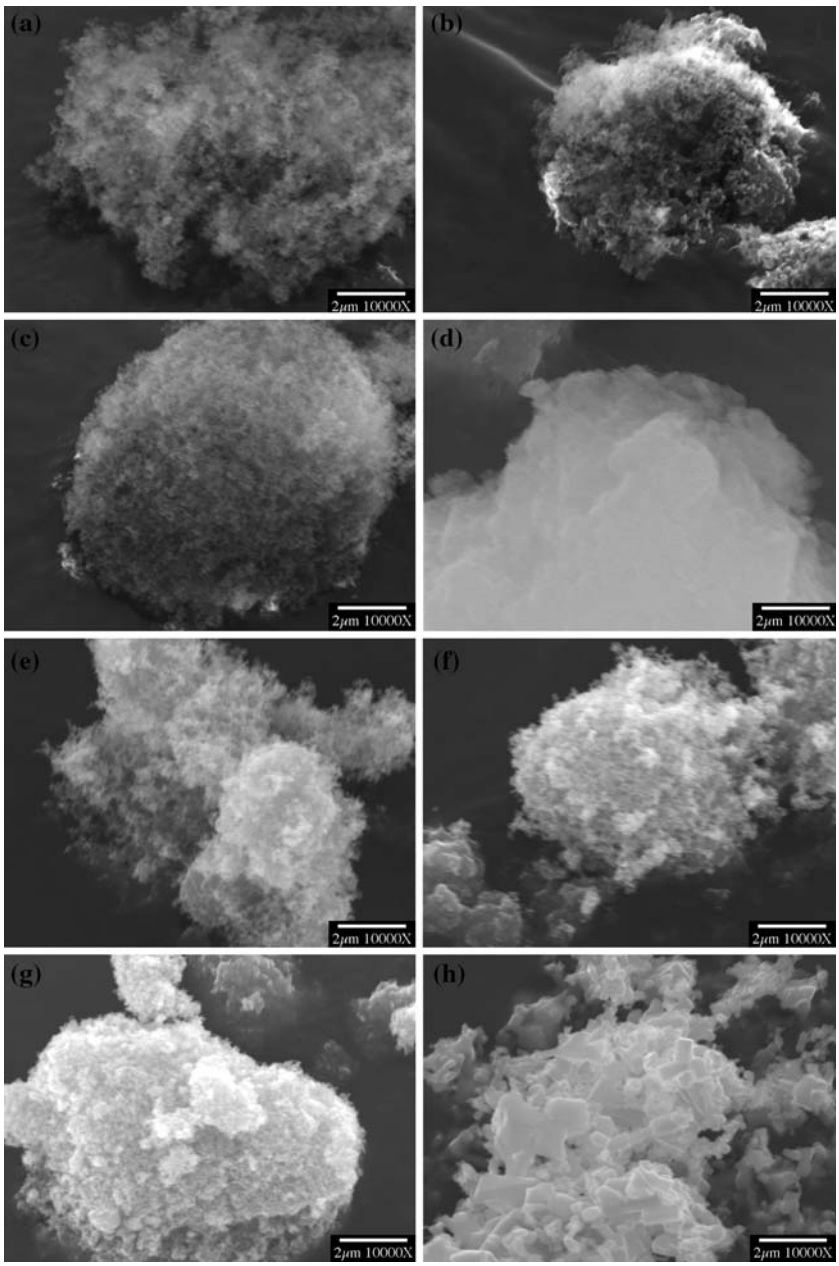

Fig. 1 Scanning electron microscope photographs of the solid components investigated. (**a**) Fumed alumina 1. (**b**) Fumed alumina 2. (**c**) Fumed alumina 2 with silane coating. (**d**) Non-fumed alumina 1. (**e**) Fumed zinc oxide. (**f**) Fumed zinc oxide with silane coating. (**g**) Non-fumed zinc oxide 1. (**h**) Non-fumed zinc oxide 2

thermal interface material. The cooling in this test is provided by a second 3 × 3 inch copper block, which is cooled by running water that flowed into and out of the block (bottom block in Fig. 1). This block is in contact with the other of the two 1 × 1 inch copper blocks that sandwich the thermal paste. The two mating surfaces of the two 1 × 1 in copper blocks are either "rough" (15 μm roughness, as attained by mechanical polishing) or "smooth" (0.009 μm roughness and 0.040–0.116 μm flatness, as attained by diamond turning). A 100-Ω resistance temperature detector (RTD) probe is inserted in four holes (T_1, T_2, T_3 and T_4 in Fig. 2, each hole of diameter 3.2 mm). Two of the four holes are in each of the 1 × 1 inch copper blocks. The temperature gradient is determined from T_1 to T_2 and T_3 to T_4. These two quantities should be equal at equilibrium, which is attained after holding the temperature of the heater at the desired value for 30 min. Equilibrium is assumed when the temperature variation is within ±0.1 °C in a period of 15 min. At equilibrium, the temperature of the hot block is in the range 70–80 °C, that of the cold block is in the range 60–40 °C, while that of the thermal paste is in the range 60–70 °C. The pressure in the direction perpendicular to the plane of the thermal interface is controlled by using a hydraulic press at pressures of 0.46, 0.69 and 0.92 MPa. The system is thermally insulated by wrapping laterally all the copper blocks with glass fiber cloth.

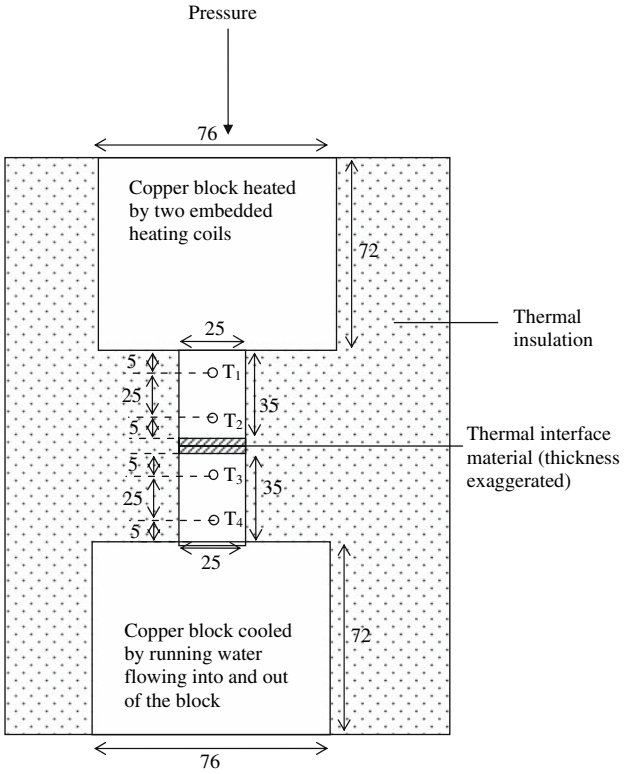

Fig. 2 A schematic representation of the steady-state method (Guarded Hot Plate Method) of thermal contact conductance measurement. T_1, T_2, T_3 and T_4 are holes of diameter 2.4 mm. A thermocouple (Type T) is inserted in each hole. All dimensions are in mm

In accordance with ASTM Method D5470, the heat flow Q is given by

$$Q = \frac{\lambda A}{d_A}\Delta T \tag{1}$$

where $\Delta T = T_1 - T_2 = T_3 - T_4$, λ is the thermal conductivity of copper, A is the area of the 1×1 in copper block, and d_A is the distance between thermocouples T_1 and T_2 (i.e., 25 mm).

The temperature at the top surface of the thermal interface material is T_A, which is given by

$$T_A = T_2 - \frac{d_B}{d_A}(T_1 - T_2) \tag{2}$$

where d_B is the distance between thermocouple T_2 and the top surface of the thermal interface material (i.e., 5 mm). The temperature at the bottom surface of the thermal interface material is T_D, which is given by

$$T_D = T_3 + \frac{d_D}{d_C}(T_3 - T_4) \tag{3}$$

where d_D is the distance between thermocouple T_3 and the bottom surface of the thermal interface material (i.e., 5 mm) and d_C is the distance between thermocouples T_3 and T_4 (i.e., 25 mm).

The thermal resistivity θ is given by

$$\theta = (T_A - T_D)\frac{A}{Q} \tag{4}$$

Note that insertion of Eq. 1 into Eq. 4 causes cancellation of the term A, so that θ is independent of A. The thermal contact conductance is the reciprocal of θ.

Bond-line thickness measurement

The bond-line thickness refers to the thickness of the thermal interface material. It is measured by sandwiching the thermal paste at a pressure of 0.46 MPa with the "rough" copper blocks used for thermal contact conductance measurement. A low value of the bond-line thickness is associated with high spreadability of the thermal paste. A strain gage mounted between the surfaces that sandwich the thermal interface material, as shown in Fig. 3, is used for the bond-line thickness measurement. The strain gage works by sensing the deformation induced by the distance change between the two mating surfaces. The bond-line thickness is calculated from the electrical output of the strain gage. The measurement is conducted at room temperature to avoid experimental error associated with the thermal expansion of the copper blocks and of the strain gage. The accuracy of this testing method is verified by the testing of copper foils of thickness 15 and 25 μm, which show an error of 15% in the thickness measurement.

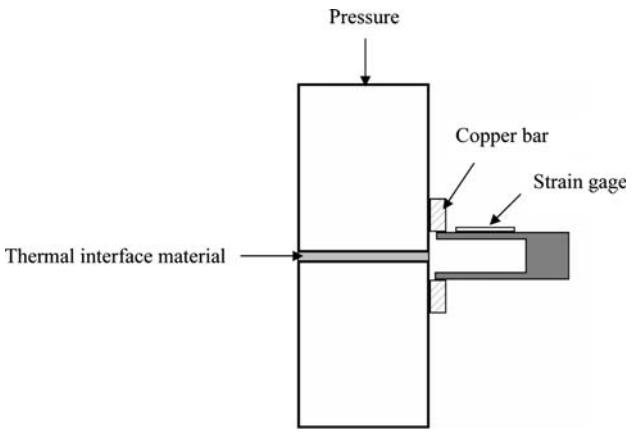

Fig. 3 A schematic representation of the bond-line thickness measurement method

Thermal stability testing

The thermal stability refers to the ability to resist elevated temperatures. It is necessary for a thermal paste to be able to resist the elevated temperatures involved in the particular application environment. The thermal stability is evaluated by measurement of the weight loss due to heating in air in a furnace at 200 °C for 24 h. The specimens are contained in aluminum weighing dishes. Three specimens of each type are tested. The heating rate and cooling rate are 3 °C/min.

Viscosity measurement

The viscosity describes the resistance to shear deformation. It is a commonly used attribute for describing pastes. The viscosity of various pastes is measured by using a viscometer (Brookfield Engineering Laboratories, Inc., Middleboro, MA, Model LVT Dial-Reading Viscometer, with Model SSA-18/13R Small Sample Adaptor). In addition, the viscometer is used to measure and the thixotropic index, as explained below.

Thixotropy refers to the rheological behavior in which a material flows only under a stress. An example of a thixotropic paste is Ketchup. The thixotropic index is a time dependent rheological property that describes the extent of thixotropic behavior. A range of rotational speeds are selected. The apparent viscosity is measured while the shear rate is progressively increased to the maximum and then progressively decreased to the minimum at constant time intervals. After the last viscosity measurement, the viscometer is turned off for 10 min. After this rest period, a measurement of the viscosity at the lowest rate is taken again. Two methods can be used to calculate the thixotropic index. Method A is the ratio of the increasing speed viscosity to that of the decreasing speed viscosity. Method B is the ratio of the lowest speed viscosity taken after the rest period to that before the rest period. The higher either ratio is, the greater is the thixotropy [18].

Phase separation testing

Commercial thermal pastes are commonly packaged in syringes to enable dispensing of the material onto a working surface. The shelf life of the paste depends on the tendency for phase separation. To test the tendency for phase separation, the pastes under study are stored in glass vials (1 dram or 1/8 oz each) at 100 °C for a period of 24 h, after which they are checked for the occurrence of phase separation by visual inspection. The pastes studied contain 4.0 vol.% filler, except fumed alumina 2 and fumed alumina with silane coating, which are at 2.4 vol.%.

Results and discussion

Thermal contact conductance and bond-line thickness

Table 2 gives the thermal contact conductance and bond-line thickness of all the pastes studied. In the case of alumina pastes with 4.0 vol.% fillers, fumed alumina 1, fumed alumina 2 and fumed alumina with silane coating are more effective than non-fumed alumina 1 and non-fumed alumina 2 as thermally conductive fillers. This result can be explained by the fluffiness of the fumed oxides and the consequent ability to be compressed and hence conform to the topography of the surfaces. These squishable fillers have a similar structure as carbon black, which has been previously shown to be effective fillers for thermal pastes [12]. The superiority of the fumed form (with silane coating) compared to the non-fumed zinc oxide form 1 and 2 is also observed for pastes containing 4.0 vol.% zinc oxide. However, the uncoated fumed zinc oxide does not show superiority over non-fumed zinc oxide 1 or non-fumed zinc oxide 2. This may be caused by the fact that the fumed zinc oxide studied is designed for hydrophilic applications, thus making its dispersion in the vehicle, which is an oil, difficult.

Comparison of the results for fumed alumina 2 (not coated, Line 3) and fumed alumina with coating (treated by octylsilane, Line 6) shows that the treatment helps the thermal conductance. The positive effect of the silane treatment is even stronger for zinc oxide (Lines 11, 12 and 13, 14). This is due to the silane treatment improving the interface between the oxide filler and the matrix, since the layer of silane changes the particle surface from being hydrophilic to being hydrophobic. The surface treatment may also reduce the interaction between particles and decrease the size and reduce the amount of particle agglomerates, which will lead to a thinner bond-line thickness of the pastes.

According to Eq. 5 below [19], a smaller bond-line thickness will give a lower thermal resistance, which means a higher thermal conductance.

$$R = t/k + R_1 + R_2 \tag{5}$$

where t is the bond-line thickness of the thermal interface material, k is the thermal conductivity of the thermal interface material, R is the total thermal resistance, and R_1 and R_2 are the thermal resistances of the interface between the thermal interface material and the two surfaces that sandwich the interface material.

The silane treatment also results in a lower viscosity of the paste (section "Viscosity"). The lower viscosity facilitates the filling of the valleys associated with the topography of the mating surfaces. A better interface between

Table 2 Thermal conductance and bond-line thickness of various thermal pastes

Line No.	Solid component		Thermal contact conductance (10^4 W/m^2 °C)					Thickness (μm)
			Rough surfaces			Smooth surfaces		
	Type	Vol.%	0.46 MPa	0.69 MPa	0.92 MPa	0.46 MPa	0.69 MPa	0.46 MPa
1	Carbon black	2.4	9.70 ± 0.11	10.23 ± 0.11	11.79 ± 0.27	25.91 ± 0.16	27.75 ± 0.14	–1.4 ± 2.6
2	Fumed alumina 1	4.0	8.36 ± 0.11	8.54 ± 0.19	9.00 ± 0.06			
3	Fumed alumina 2	4.0	6.92 ± 0.29	7.80 ± 0.21	8.03 ± 0.29	/	/	/
4	Fumed alumina with silane coating	1.2	9.69 ± 0.18	10.00 ± 0.19	10.13 ± 0.10	/	/	/
5		2.4	10.00 ± 0.24	10.55 ± 0.28	10.52 ± 0.27	25.13 ± 0.76	27.76 ± 0.25	–2.0 ± 3.4
6		4.0	8.70 ± 0.12	9.42 ± 0.07	9.41 ± 0.04	/	/	/
7		6.0	8.17 ± 0.12	8.32 ± 0.19	8.43 ± 0.12	/	/	/
8		10.0	7.16 ± 0.10	7.34 ± 0.07	7.10 ± 0.11	/	/	3.8 ± 2.2
9	Non-fumed alumina 1	4.0	3.15 ± 0.03	/	/	/	/	/
10	Non-fumed alumina 2	4.0	1.41 ± 0.01	/	/	/	/	/
11	Fumed zinc oxide	2.4	5.44 ± 0.04	6.10 ± 0.18	6.75 ± 0.10	/	/	/
12		4.0	6.28 ± 0.11	6.59 ± 0.14	6.87 ± 0.20	/	/	/
13	Fumed zinc oxide with silane coating	2.4	10.01 ± 0.29	10.66 ± 0.12	11.02 ± 0.09	/	/	/
14		4.0	10.10 ± 0.20	10.80 ± 0.22	11.12 ± 0.26	20.30 ± 0.17	25.22 ± 0.87	–0.8 ± 1.8
15		6.0	9.25 ± 0.11	9.54 ± 0.15	9.74 ± 0.13	/	/	/
16		10.0	9.10 ± 0.15	9.47 ± 0.39	9.61 ± 0.64	/	/	/
17		16.0	9.19 ± 0.07	9.42 ± 0.10	9.66 ± 0.13	18.95 ± 0.28	21.65 ± 0.11	3.3 ± 0.8
18		20.0	8.55 ± 0.17	9.51 ± 0.02	9.68 ± 0.06	/	/	/
19		30.0	2.97 ± 0.04	/	/	/	/	22.4 ± 4.4
20	Non-fumed zinc oxide 1	2.4	6.57 ± 0.08	6.89 ± 0.07	7.67 ± 0.17	/	/	/
21		4.0	6.32 ± 0.10	6.89 ± 0.05	7.12 ± 0.08	17.02 ± 0.14	19.98 ± 0.15	/
22		6.0	5.65 ± 0.05	5.96 ± 0.03	6.69 ± 0.08	/	/	/
23	Non-fumed zinc oxide 2	4.0	7.89 ± 0.15	8.10 ± 0.04	8.51 ± 0.17	15.34 ± 0.14	16.90 ± 0.44	/
24	Titanium dioxide	4.0	6.12 ± 0.12	6.33 ± 0.06	6.61 ± 0.02	/	/	/
25	None	0.0	10.50 ± 0.60	10.70 ± 0.10	11.30 ± 0.20	28.79 ± 0.16	32.72 ± 1.62	/
26	Ceramique [9]		7.21 ± 0.10	8.47 ± 0.53	9.92 ± 0.41	21.48 ± 1.12	24.10 ± 0.76	/
27	Shin-Etsu		7.76 ± 0.14	8.43 ± 0.20	8.78 ± 0.11	19.87 ± 0.27	22.55 ± 0.43	27.3 ± 5.2

Negative values of the bond-line thickness are due to the error in measuring small thickness values

the paste and the mating surface can reduce the contact resistance, thus resulting in a lower value of the total thermal resistance, as shown by Eq. 5.

The optimized composition of the silane coated fumed alumina paste is 2.4 vol.% filler, with 97.6 vol.% vehicle, as this gives the highest conductance, at least for the case of the rough surfaces. The optimized composition of the fumed zinc oxide with silane coating paste is 4.0 vol.% filler, with 96 vol.% vehicle. Both of these optimized pastes have essentially thermal conductance values that are higher than those of commercial products, namely Ceramique and Shin-Etsu. For the case of smooth surfaces, the optimized pastes are also more effective than the two commercial products.

Comparison of the optimized fumed oxide pastes (2.4 vol.% silane coated fumed alumina and 4.0 vol.% silane coated fumed zinc oxide) with the commercial Shin-Etsu product shows that the bond-line thicknesses of the two pastes are much lower than that of Shin-Etsu. This explains why the thermal contact conductance of Shin-Etsu is lower than the optimized fumed oxide pastes, though it has a high thermal conductivity of 6.0 W/m K, as reported by Shin-Etsu.

Table 2 shows that fumed titanium dioxide is not as effective as fumed alumina or fumed zinc oxide. This is probably because of its relatively low thermal conductivity (6.69 W/m K) [20] and its hydrophilic surface condition, which leads to poor dispersion.

For the vehicle in the absence of a solid component (Line 25 of Table 2), the thermal contact conductance is higher than any of the other cases in the table, whether the mating surfaces are rough or smooth. In other words, the addition of any of the solid components causes the thermal contact conductance to decrease, although it tends to

increase the thermal conductivity within the thermal interface material. This is believed to be due to the very low bond-line thickness attained when there is no solid component. On the other hand, the viscosity is very low in the absence of a solid component (section "Viscosity"). A very low viscosity is undesirable in relation to the tendency for seepage and the difficulty of footprint control during application.

Viscosity

The viscosity of selected pastes and the unfilled vehicle are shown in Fig. 4. The presence of a solid component (filler), whichever type, increases the viscosity. At the same solid component content of 2.4 vol.%, fumed alumina 2 gives much higher viscosity than the silane coated fumed alumina, probably because the silane coating decreases the interaction between the alumina aggregates, thereby decreasing the shear stress required to break the flocculation. A similar effect of silane coating is observed for the zinc oxide paste. A lower viscosity is expected to increase the spreadability, hence decreasing the thermal resistance, as explained in section "Thermal contact conductance and bond-line thickness".

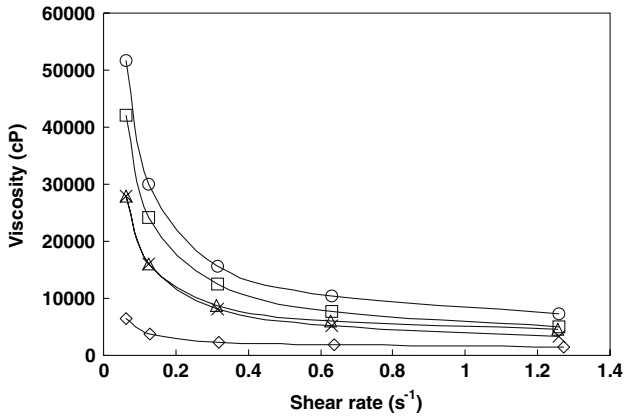

Fig. 4 Effect of shear rate on the viscosity for pastes with alumina or zinc oxide. □: 4 vol.% fumed zinc oxide; Δ: 4 vol.% fumed zinc oxide with silane coating: ○: 2.4 vol.% fumed alumina 2; × : 2.4 vol.% fumed alumina with silane coating; ◇: 100% vehicle

The thixotropic index, as shown in Table 3, decreases in the presence of a solid component. This behavior is associated with a slow recovery process after the application of shear, although the breakdown upon shear is rapid. Table 3 shows that the thixotropic index determined by using Method A is comparable to that determined by Method B. Table 3 also shows that adding fumed oxides increases the shear-thinning index. Shear thinning (i.e., the decrease of viscosity with increasing shear rate) can be attributed to the particles becoming more aligned and hence less entangled and less resistant to deformation as the shear rate is increased.

Some filled polymer systems can be modeled as power law fluids [21]. A simple calculation based on the viscosity data in Fig. 4 and using Eq. 6 below shows that the thermal pastes studied obey the power law fluids model.

$$\eta = K(\dot{\gamma})^{n-1} \tag{6}$$

In Eq. 6, K is the consistency index, n is power law index and $\dot{\gamma}$ is the strain rate. Figure 5 shows a linear relationship in the plot of log η versus log $\dot{\gamma}$ for all types of thermal

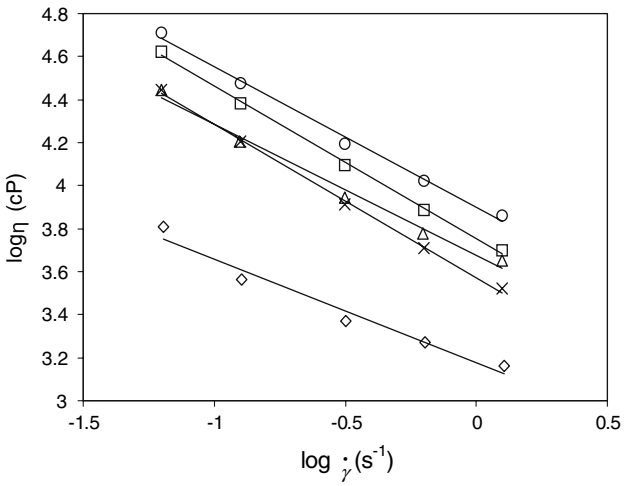

Fig. 5 Power-law model fitting of the dependence of the viscosity on the shear strain rate for pastes with and without a solid component (alumina or zinc oxide). □: 4 vol.% fumed zinc oxide; Δ: 4 vol.% fumed zinc oxide with silane coating: ○: 2.4 vol.% fumed alumina 2; × : 2.4 vol.% fumed alumina with silane coating; ◇: 100% vehicle

Table 3 Shear-thinning index and thixotropic index of selected thermal pastes

Solid component	Shear-thinning index	Thixotropic index	
		Method A	Method B
None	3.44	1.35	1.35
4 vol.% fumed zinc oxides with silane coating	4.66	0.78	0.89
4 vol.% fumed zinc oxide	5.44	0.91	0.91
2.4 vol.% fumed alumina with silane coating	5.47	0.95	0.92
2.4 vol.% fumed alumina 2	4.90	0.99	0.93

pastes studied. The fitted equations and the derived rheological parameters, n and K, are listed in Table 4. The rheological parameter K reflects the consistency of the filled polymer, with higher values representative of more viscous materials [21]. The rheological parameter n is the power-law index that gives a measure of the pseudo-plasticity, with greater departures from unity corresponding to more pronounced shear-thinning behavior [21]. This means that the results of the power-law model fitting are consistent with the trend in the viscosity (Fig. 4) and with the trend in the shear-thinning index (Table 3).

Thermal stability

The thermal stability testing results, as shown in Table 5 are expressed in terms of the fractional residual weight including the solid component and that excluding the solid component. The latter is more indicative of the thermal stability of the liquid in the paste, whereas the former includes the effect of the filler volume fraction.

Comparison of Lines 1, 2, 3 and 6 shows that the presence of the alumina essentially does not affect the thermal stability calculated by excluding the solid component. All the three types of the alumina give similar results in thermal stability, though their morphology is different. Comparison of Lines 3 and 4 shows that the silane coating enhances the thermal stability, whether the fractional residual weight is calculated by including the solid component or not. Comparison of Lines 4 and 5 shows that increasing the volume fraction of fumed alumina (with silane coating) does not enhance the thermal stability.

Similarly, all the types of zinc oxide without surface treatment show almost the same thermal stability performance, though they have different morphologies and are from different sources. The silane coating also enhances

Table 4 Fitted equation and derived rheological parameters of selected thermal pastes

Solid component	Fitted equation	R^2*	n	K
None	Log η = –0.48 log $\dot{\gamma}$ + 3.18	0.969	0.52	1502.45
4 vol.% fumed zinc oxide with silane coating	Log η = –0.61 log $\dot{\gamma}$ + 3.67	0.998	0.39	4716.29
4 vol.% fumed zinc oxide	Log η = –0.71 log $\dot{\gamma}$ + 3.75	0.998	0.29	5675.45
2.4 vol.% fumed alumina with silane coating	Log η = –0.71 log $\dot{\gamma}$ + 3.57	0.994	0.29	3749.73
2.4 vol.% fumed alumina 2	Log η = –0.66 log $\dot{\gamma}$ + 3.90	0.987	0.34	7912.25

*R^2 (R-squared value, also known as the coefficient of determination) is a statistical measure of how well a regression line approximates the real data points. The closer it is to one, the greater is the ability of the fitted equation to predict the linear trend

Table 5 Thermal stability of various thermal pastes, as shown by the residual mass after heating, with the mass of the solid component either excluded or included

Line No.	Solid component	Solid component (vol.%)	Vehicle (vol.%)	Residual (wt.%)	
				Excluding the solid component	Including the solid component
1	None	0	100	31.2 ± 1.0	31.2 ± 0.7
2	Fumed alumina 1	4.0	96.0	31.4 ± 0.6	20.8 ± 0.7
3	Fumed alumina 2	4.0	96.0	27.7 ± 1.8	18.7 ± 2.0
4	Fumed alumina with silane coating	4.0	96.0	45.3 ± 1.3	39.1 ± 1.4
5	Fumed alumina with silane coating	10.0	90.0	45.9 ± 0.7	29.8 ± 0.7
6	Non-fumed alumina 1	4.0	96.0	32.7 ± 0.5	22.3 ± 0.6
7	Fumed zinc oxide	4.0	96.0	59.4 ± 1.9	49.6 ± 2.3
8	Fumed zinc oxide with silane coating	4.0	96.0	67.6 ± 1.0	59.7 ± 1.2
9	Fumed zinc oxide with silane coating	16.0	84.0	81.6 ± 0.4	61.4 ± 0.8
10	Non-fumed zinc oxide 1	4.0	96.0	55.9 ± 2.0	45.2 ± 2.4
11	Non-fumed zinc oxide 2	4.0	96.0	59.7 ± 1.2	50.0 ± 1.5
12	Titanium dioxide	4.0	96.0	54.0 ± 1.2	47.0 ± 1.3

the thermal stability of zinc oxide pastes, as shown by comparing Lines 7 and 8.

The origin of the effect of the silane coating on the thermal stability is presently unclear. However, it may be due to the layer of silane on the particle surface hindering the interaction of the surface with the vehicle.

Comparison of the pastes with alumina and those with zinc oxide shows that the latter exhibits better thermal stability performance. This is probably caused by the pH of the particles, since the pH value of alumina is 3.0–5.0, while zinc oxide is amphoteric, with its pH at 6.5–8.0.

Phase separation

The photographs taken by a digital camera of the pastes after phase separation testing are shown in Fig. 6. Among the alumina pastes, the non-fumed alumina 1 paste (Sample A in Fig. 6) exhibits the most serious separation, and the non-fumed alumina 2 paste (Sample B) also shows quite serious separation, while the fumed alumina 2 paste (Sample C) and fumed alumina (with silane coating) paste (Sample D) do not show any observable separation. Among the zinc oxides pastes, both the non-fumed zinc oxide 2 paste (Sample E) and the non-fumed zinc oxide 1 paste (Sample F) suffer from serious phase separation, while pastes containing fumed zinc oxide with or without silane coating (Samples G and H) show slight phase separation. The higher tendency for separation for fumed zinc oxide than fumed alumina is mainly due to the relatively high density of zinc oxide. Increase of the volume fraction of the filler will diminish the phase separation; for example, there is no observable separation for the paste with 16.0 vol.% silane coated fumed zinc oxide (photo not shown here). The effectiveness of fumed oxides for enhancing the resistance to phase separation is due to their porous fluffy structure, which helps form a network and hold the vehicle.

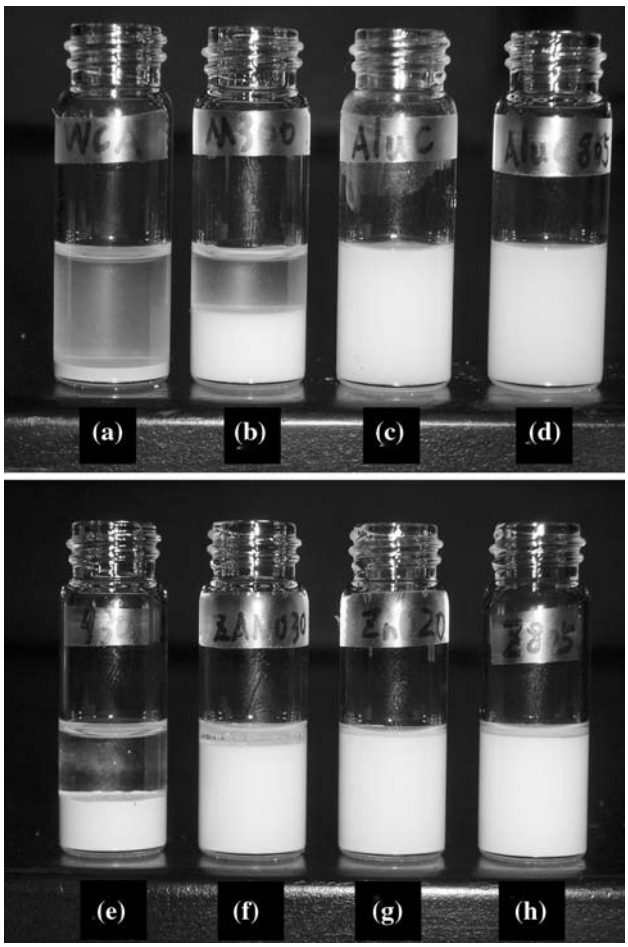

Fig. 6 Phase separation behavior of selected thermal pastes. (**a**) 4.0 vol.% non-fumed alumina 2; (**b**) 4.0 vol.% non-fumed alumina 1; (**c**) 2.4 vol.% fumed alumina 2; (**d**) 2.4 vol.% fumed alumina with silane coating; (**e**) 4.0 vol.% non-fumed zinc oxide 2; (**f**) 4.0 vol.% non-fumed zinc oxide 1; (**g**) 4.0 vol.% fumed zinc oxide; (**h**) 4.0 vol.% fumed zinc oxide with silane coating

Conclusion

Nanostructured fumed metal oxides (aluminum oxide of particle size 13 nm and zinc oxide of particle size 20–25 nm), which are in the form of porous agglomerates of nanoparticles, are highly effective as thermally conductive solid components in thermal pastes. They are as effective as previously reported carbon black, but are advantageous in their electrical non-conductivity. Without fuming, the oxides are less effective. The nanoparticles allow effective filling of the microscopic valleys in the surface topography of the mating surfaces, while the porous agglomerate structure associated with the fumed form allows the solid component to be highly compressible (squishable). By coating with silane prior to use, both fumed alumina and fumed zinc oxide become even more effective. The silane coating decreases the viscosity of the paste. The thixotropic index is decreased by the presence of an oxide as the solid component, while the shear-thinning index is increased. The fumed titanium dioxide is less effective than alumina or zinc oxide (whether fumed or not).

The organic vehicle (polyol esters) and solid component content (2.4–4.0 vol.%) are chosen to allow the pastes to be highly conformable and spreadable. The spreadability results in a small bond-line thickness, which helps reduce the thermal resistance. Fumed metal oxide volume fractions beyond 4.0 vol.% give thermal pastes that are less effective, with lower values of the thermal contact conductance and higher values of the bond-line thickness.

The thermal contact conductance is even higher when no solid component is present at all. However, the associated viscosity is very low, causing difficulty in practical use.

The effectiveness of thermal pastes is evaluated by measuring the thermal contact conductance across copper mating surfaces of controlled roughness levels and at controlled pressures, using the Guarded Hot Plate Method. The use of either 4.0 vol.% silane coated fumed zinc oxide or 2.4 vol.% silane coated alumina in the polyol ester vehicle gives thermal pastes that are more effective than commercial thermal pastes (Ceramique and Shin-Etsu) when the mating surfaces have a surface roughness of 15 μm. These fumed oxide pastes are comparable to or more effective than these commercial thermal pastes when the mating surfaces have a surface roughness of 0.009 μm. The bond-line thickness at a pressure of 0.46 MPa is less than 3 μm for the oxide pastes, but is 27 μm for the commercial Shin-Etsu paste.

The residual weight (excluding the weight of the solid component) of the paste after heating at 200 °C for 24 h is increased from 31% in the absence of a solid component to 45% in the presence of 2.4 vol.% silane coated fumed alumina, and to 68% in the presence of 4.0 vol.% silane coated fumed zinc oxide. Fumed zinc oxide is superior to non-fumed zinc oxide in improving the thermal stability. Silane coating of the fumed zinc oxide further improves the thermal stability. Fumed alumina does not affect the thermal stability, but silane coated fumed alumina improves the thermal stability.

Though silane coated fumed zinc oxide is superior to silane coated alumina in enhancing the thermal stability, it is inferior in the phase separation tendency. However, the phase separation tendency is low for both pastes.

References

1. Wolff EG, Schneider DA (1998) Int J Heat Mass Transfer 41:3469
2. Ouellette T, de Sorgo M (1985) Proc. Power Electron. Des. Conf. Power Sources Users Conference, Cerritos, CA, 134
3. Vogel MR (1995) Advances in electronic packaging, Proc. Int. Intersociety Electron. Packag. Conf., American Society of Mechanical Engineers, New York, NY, vol 10-2, p 989
4. Sartre V, Lallemand M (2001) Appl Therm Eng 21:221
5. Grujicic M, Zhao CL, Dusel EC (2005) Appl Surf Sci 246:290
6. Chung DDL (2001) J Mater Eng Performance 10:56
7. Xu Y, Luo X, Chung DDL (2002) J Electron Packaging 124:188
8. Leong C-K, Chung DDL (2003) Carbon 41:2459
9. Leong C-K, Chung DDL (2004) Carbon 42:2323
10. Leong C-K, Aoyagi Y, Chung DDL (2006) Carbon 44(3):435
11. Howe TA, Leong C-K, Chung DDL (2006) J Electron Mater 35(8):1628
12. Leong C-K, Aoyagi Y, Chung DDL (2005) J Electron Mater 34(10):1336
13. Gaydardzhiev S, Ay P (2006) J Mater Sci 41(16):5257
14. Batz-Sohn C (2003) Part Part Syst Char 20(6):370 (Volume Date 2004)
15. Gun'ko VM, Zarko VI, Leboda R, Chibowski E (2001) Adv Colloid Interface Sci 91(1):1
16. Mun JH, Sim IC (2002) Republ. Korean Kongkae Taeho Kongbo KR 2002060926
17. Kim BM (2002) Republ. Korean Kongkae Taeho Kongbo KR 2002061469
18. De Kretser RG, Scales PJ, Boger DV (1998) Colloid Surface A 137:307
19. Prasher R (2001) J Heat Transfer 123:969
20. Alexander W, Shackelford J (2001) CRC materials science and engineering handbook. CRC Press LLC, Boca Raton, FL, USA, p 284
21. Shenoy AV (1999) Rheology of filled polymer systems. Kluwer Academic Publishers, Norwell, MA, USA, p 80